Journal of Medicinal Chemistry

Article

Identification, Characterization and Optimization of 2,8-Disubstituted-1,5-naphthyridines as Novel Plasmodium falciparum Phosphatidylinositol-4-kinase Inhibitors with in Vivo Efficacy in a Humanized Mouse Model of Malaria

Nishanth Kandepedu, Diego Gonzalez Cabrera, Srinivas Eedubilli, Dale Taylor, Christel Brunschwig, Liezl Gibhard, Mathew Njoroge, Nina Lawrence, Tanya Paquet, Charles J Eyermann, Thomas Spangenberg, Gregory S. Basarab, Leslie J. Street, and Kelly Chibale

J. Med. Chem., **Just Accepted Manuscript** • DOI: 10.1021/acs.jmedchem.8b00648 • Publication Date (Web): 11 Jun 2018

ACS Publications

is published by the American Chemical Society. 1155 Sixteenth Street N.W., Washington, DC 20036

Identification, Characterization and Optimization of 2,8-Disubstituted-1,5-naphthyridines as Novel *Plasmodium falciparum* Phosphatidylinositol-4-kinase Inhibitors with in Vivo Efficacy in a Humanized Mouse Model of Malaria

Nishanth Kandepedu[†], Diego Gonzàlez Cabrera[†], Srinivas Eedubilli[†], Dale Taylor[∞], Christel Brunschwig[∞], Liezl Gibhard[∞], Mathew Njoroge[∞], Nina Lawrence[∞], Tanya Paquet[†], Charles J. Eyermann[†], Thomas Spangenberg[¥], Gregory S. Basarab[†], Leslie J. Street[†] and Kelly Chibale[*,†,#]

[†]Drug Discovery and Development Centre (H3D), University of Cape Town, Rondebosch 7701, South Africa; [∞]Drug Discovery and Development Centre (H3D), DMPK/Pharmacology, University of Cape Town, Observatory, 7925, South Africa; [¥]Merck Global Health Institute, Ares Trading S.A., a subsidiary of Merck KGaA (Darmstadt, Germany), Coinsins 1267, Switzerland; [#]South African Medical Research Council, Drug Discovery and Development Research Unit, Department of Chemistry and Institute of Infectious Disease and Molecular Medicine, University of Cape Town, Rondebosch 7701, South Africa.

ABSTRACT

A novel 2,8-disubstituted-1,5-naphthyridine hit compound stemming from the open access Medicines for Malaria Venture Pathogen Box, formed a basis for a hit-to-lead medicinal chemistry program. Structure-activity relationship investigations resulted in compounds with potent antiplasmodial activity against both chloroquine sensitive (NF54) and multi-drug resistant (K1) strains of the human malaria parasite *Plasmodium falciparum*. In the

humanized *P. falciparum* mouse efficacy model, one of the frontrunner compounds showed in vivo efficacy at an oral dose of 4 × 50 $mg.kg^{-1}$. In vitro mode-of-action studies revealed *Plasmodium falciparum* phosphatidylinositol-4-kinase as the target.

INTRODUCTION

Malaria represents a major global health burden with an estimated 216 million new cases and nearly 445000 deaths in 2016, mostly affecting young children and pregnant women.[1] It is a vector-borne infectious disease caused by the hematoprotozoan parasite of genus *Plasmodium*.[2] According to the recent data from the World Health Organization (WHO),[1] *Plasmodium falciparum* was responsible for 99% of the malaria related morbidity and mortality in sub-Saharan Africa, whereas, *Plasmodium vivax* caused 36% of malarial infections in the rest of the world.

Currently, the WHO recommended artemisinin-based combination therapy (ACT) and vector control measures are key players in relieving the malarial burden.[1,3] However, recent reports of emerging resistance towards ACTs,[4] and the availability of a limited number of validated drug targets exemplified by dihydrofolate reductase, cytochrome *c*-oxidoreductases and hemozoin formation,[5] emphasises the need to expand chemical matter towards more efficacious drugs with novel modes of action and multi-stage antiparasitic activity. Within this context, *Plasmodium* kinases are attractive targets for new generation antimalarials as both protein and lipid kinases are involved in key signalling pathways at various stages of the parasite lifecycle and have had some level of genetic or phenotypic validation.[6] Even though, to our knowledge, there has yet not been any inhibitor(s) of *Plasmodium* protein kinases (PKs) in human clinical trials, substantial knowledge pertaining to the validity of PKs as drug targets has been obtained using genoproteomic approaches.[7] On the other hand, lipid kinases are important in all stages of the *Plasmodium* lifecycle; this includes phosphatidylinositol-4-

kinase (PI4K) that catalyses the conversion of phosphatidylinositol (PI) to phosphatidylinositol-4-phosphate (PI4P).[8,9] *Plasmodium* PI4K is therefore important for signal transduction and membrane trafficking and has been shown to be a validated drug target for prevention, treatment, and elimination of malaria.[9] The 2-aminopyridine MMV390048 was recently reported as a *Plasmodium* PI4K inhibitor[10] and is currently in Phase IIa clinical trials,[11] and several other published antimalarials including BQR695, KDU691, BRD73842 also target *Plasmodium* PI4K (Figure 1).[9,12] The series presented herein also inhibits PI4K, thus offering a new chemotype to interrogate this important new antimalarial target. However, none of the known PI4K inhibitors have yet cleared the clinical phase of development and are available to patients.

Medicines for Malaria Venture (MMV) has assembled a set of small molecules termed the Pathogen Box,[13] containing 400 open-source drug-like compounds that are active against neglected diseases[14-16] from which the previously unexplored 1,5-naphthyridine MMV024101 (**8**, Figure 2), active on *P. falciparum* with a described *Pf*3D7 IC_{50} of 600 nM was selected as a starting point for our medicinal chemistry campaign. When resynthesized for validation, **8** showed submicromolar potency against *P. falciparum* NF54 (IC_{50} = 543 nM), low aqueous solubility (<5 μM) and rapid clearance by mouse liver microsomes with only 2% of parent compound remaining after 30 minutes of incubation. In order to address these shortcomings, we explored substitutions at both the 2- and 8-positions of the 1,5-naphthyridine scaffold to identify a drug-like candidate with an overall improved Absorption, Distribution, Metabolism, and Excretion (ADME) profile. Herein, we report the synthesis, in vitro antiplasmodial activity, and ADME profiles of a selection of 1,5-naphthyridines. A representative compound **55**, with low nanomolar in vitro antiplasmodial activity, good ADME and oral pharmacokinetic (PK) properties, was tested for in vivo efficacy in the NOD-scid IL2Rγ^{null} (NSG) murine malaria disease model of *P. falciparum* infection, in the

recently established *Pf*SCID platform at the University of Cape Town. In addition, three compounds (**21**, **26**, and **30**) were used to determine the mode-of-action of the 1,5-naphthyridine series and were contextualized with other *P. falciparum* PI4K inhibitors.

RESULTS AND DISCUSSION

Chemistry. Target compounds **8-55** were synthesized using a linear synthetic route starting from commercially available 6-methoxypyridin-3-amine (Scheme 1). The key intermediate **4** was synthesized using a previously reported procedure.[17] Briefly, the first step involves condensation of **1** with Meldrum's acid and trimethoxymethane. The domino sequence includes an addition-elimination reaction to form the enamine intermediate **2** that, in the subsequent step, undergoes thermal cyclization with decarboxylation to form **3**. A facile bromination of **3** at 0 °C resulted in 8-bromo-2-methoxy-1,5-naphthyridine **4**, a key intermediate that enabled investigation of the structural changes at R^1 (position 8 of the 1,5-naphthyridine ring). This intermediate was either subjected to a Suzuki cross coupling reaction[18] or nucleophilic aromatic substitution using commercially available boronates or amines, respectively, to give compound **5**. The intermediate **5** was subjected to demethylation to form **6**, which upon a second bromination gave **7**. Intermediate **7** was then subjected either to a second Suzuki or an amination reaction using boronates or amines respectively, to furnish target compounds **8-55 (Tables 1-4)**. Commercially available aryl boronates were used in almost all the Suzuki reactions. When unavailable, boronates were synthesized using classical Miyaura borylation from the corresponding halogenated substrates.[19]

In vitro antiplasmodial activity. All synthesized compounds were tested for in vitro growth inhibition activity against a drug sensitive strain of *P. falciparum*, NF54, and selected compounds were tested for activity against a multi-drug resistant strain, K1, with chloroquine and artesunate as positive controls. Compounds with good antiplasmodial activity (IC_{50}'s

<200 nM) were also evaluated for in vitro mammalian cytotoxicity in the Chinese Hamster Ovary (CHO) cell line, using emetine as a positive control. The preliminary structure-activity relationship (SAR) investigation was focused on identifying substituents at the 2- and 8-positions of the 1,5-naphthyridine ring that gave potent antiplasmodial activity (Table 1). At R^1, the general SAR trend showed that pyridine analogues (**15-19**) displayed improved activity compared to other heterocyclic substituents like pyrazole **(8, 9)**, phenyl **(10-14)** and piperazine **(20-22)**. Both 3- and 4-linked pyridines (**16**, **17**) were equally potent and small substitutions on the pyridine rings (**18, 19**) were tolerated.

For optimization of antiplasmodial activity, by making changes at the 2-position of the 1,5-naphthyridine ring, the analogue with the 4-pyridyl group at position 8 of the scaffold was synthesized first and maintained for matched pair analyses (Table 2). This work was facilitated by the synthetic accessibility of multi-gram quantities of the required pyridine precursor, intermediate **5**. As can be seen in Tables 1 and 2, replacing the pyridine sulfonamide at the 2-position of the naphthyridine ring (R^2), e.g. compound **8** (NF54 IC_{50} = 543 nM) and compound **15** (NF54 IC_{50} = 377 nM), with phenyl sulfonamide in the *meta*-position as in compound **9** (NF54 IC_{50} = 277 nM) and **16** (NF54 IC_{50} = 122 nM), improved the NF54 activity 2- to 3-fold. *Ortho*- and *para*- phenyl sulfonamides diminished NF54 activity for compounds **23**, **24** and **31** (IC_{50}'s >5000 nM). The carboxamide, as in compound **37**, was not as well-tolerated (NF54 IC_{50} = 745 nM) compared to the sulfonamide matched pair, compound **16**. Overall, aryl carboxamides **37-41** and amines **27**, **43-45** at R^2 displayed diminished antiplasmodial activity.

As shown in Table 1 and 2, cross-resistance against K1 was not observed for the compounds tested. Compounds **16**, **26**, **28**, **29**, **30**, **35** were also assayed for cytotoxicity using CHO cells. The CHO CC_{50}/NF54 IC_{50} selectivity indices (SI) were greater than 100-fold,

except in the case of compounds **16** and **29**, where the SI values were 16-fold and 85-fold respectively. In vitro cytotoxicity indications were thus compound specific and not an intrinsic issue for the series.

Some of the noteworthy analogues identified from the SAR investigations include compounds **26** (NF54/K1 IC_{50} = 87/110 nM), **30** (NF54/K1 IC_{50} = 22/19 nM) and **35** (NF54/K1 IC_{50} = 31/65 nM). In addition, **30** showed good aqueous solubility at pH 6.5 (115 μM). However, incubation of the compound with human, mouse and rat liver microsomes revealed moderate clearance (Table 2), which needed improving.

Compounds **21** and **26** were screened for off-target inhibitory activity against a panel of 140 human protein kinases at a concentration of 10 μM. The 11% hit rate (<30% residual activity at 10 μM), suggested that these analogues have low promiscuity for human kinases. (Supporting Information Table S3) and supported continued progression of the series.

SAR exploration around compound 30. Phenyl sulfonamide analogues at the 2-position of the 1,5-naphthyridine ring showed that antiplasmodial activity could be ameliorated with larger substituents as in compounds **30** and **35**. Further SAR studies were focused at the 2-position towards improving drug metabolism and pharmacokinetic (DMPK) properties of **30** (Table 3). With the exception of the *alpha*-methyl analogue **46**, all the analogues showed good potency against NF54 with IC_{50}'s less than or equal to 200 nM. Compounds **48**, **51**, **52**, and **53** displayed higher potency (NF54 IC_{50}'s ≤50 nM) and the analogues containing a piperazine ring (**51**), a morpholine ring (**52**) or a pyrrolidine ring (**53**) showed higher aqueous solubility (>150 μM) with only **53** showing comparable metabolic stability to **30**.

Metabolite identification studies on **30** (Supporting information Section 8) supported the fact that the sulfonamide moiety was the major metabolic soft spot in mice and mouse

liver microsomes, with *N*-dealkylation producing the unsubstituted sulfonamide **16**. To mitigate the risk of CYP inhibition due to the presence of the pyridine ring,[20] and in order to explore SAR at the 8-position of the naphthyridine ring, compounds **54** and **55**, in which a trifluoromethyl group was incorporated at the 2-position of the pyridine ring, were synthesized.[21] Although compound **54** showed good potency (NF54/K1 IC_{50} = 20/46 nM) and aqueous solubility (145 μM), it displayed poor microsomal stability, suggesting that the substituted sulfonamide group remained a metabolic liability. The unsubstituted sulfonamide **55**, showed good antiplasmodial activity (NF54/K1 IC_{50} = 63/102 nM) and good microsomal stability in human, mouse, and rat liver microsomes (Table 4). Metabolic soft spots were blocked as confirmed by metabolite identification studies in mice, where only a minor oxidation metabolite of **55** occurring on the naphthyridine core or, on the pyridine substituent, was detected (Supporting Information Section 8).

The partition coefficient, log $D_{7.4}$'s of selected compounds ranged from moderate to high (1.8 to 4.2) (Supporting Information Table S1). During the course of the program, several compounds in the series were evaluated for inhibition of CYP450's and for activity against the *h*ERG K^+ channel. Compound **30** showed no inhibition of several CYP450's at 20 μM (Table 5). Four compounds **19**, **30**, **35**, and **55** were profiled for potential cardiotoxicity (*h*ERG) liabilities (Table 6). With the exception of **35**, all compounds were clean against *h*ERG (IC_{50} >10 μM), suggesting that a potential cardiotoxicity risk is not associated with the series. This is especially gratifying since the cell line used for the assay overexpresses the *h*ERG channel relative to cardiomyocytes. Based on the aggregate of antiplasmodial activity, microsomal stability and in vitro safety, compounds **30** and **55** were chosen for further profiling towards demonstrating in vivo proof-of-concept (PoC).

Gametocytocidal activity. The potential of the 1,5-naphthyridine class to behave as dual-active antimalarials was evaluated by testing **55** against gametocyte stages of the malaria parasite. A single concentration of 1 μM of **55** displayed 42% inhibition of early stage and 51% inhibition of late stage gametocytes as demonstrated by decreased activity of *Plasmodium* lactate dehydrogenase. The gametocytocidal activity of compound **55** suggests that the 1,5-naphthyridine class of compounds are more potent against asexual blood stage parasites compared to sexual gametocyte stage parasites. This observation is consistent with what has been noted for other PI4K inhibitors.[10]

Pharmacokinetic studies. When dosed intravenously, **30** was cleared quickly from blood (90 $mL.min^{-1}.kg^{-1}$). Tissue distribution was high (25.7 $L.kg^{-1}$) and half-life was moderate (3.3 h) (Table 7). A comparative oral pharmacokinetic study of **30** between mice pre-treated with 1-aminobenzotriazole (ABT, a non-selective CYP inhibitor),[22] and untreated mice, was carried out to ascertain whether or not the oral exposure of the compound could be improved and metabolism of **30** into the less active metabolite **16** minimized. Without ABT, **30** was absorbed quickly (T_{max} of 0.5 h), but, the oral exposure was low with an oral bioavailability of 8%. Exposure of the metabolite **16** was 10-fold the exposure of the parent **30**, but with a short half-life (1.6 h). ABT did partially inhibit the biotransformation of **30** into **16,** with a 2-fold increase and 2-fold decrease of the oral exposure of the parent and metabolite, respectively. As a result, the oral bioavailability of **30** did not improve significantly (15%). In fact, ABT is known to inhibit CYP enzymatic activity but not completely.[23] These results suggested that metabolism was not the only limiting factor with respect to oral exposure of **30** and that other clearance mechanisms were involved. As **16** was about 6-fold less active than **30**, it was not expected to contribute significantly to the pharmacodynamic profile of **30**, and the latter was not progressed to efficacy studies.

When dosed intravenously, **55** was cleared slowly from systemic circulation (11 $mL.min^{-1}.kg^{-1}$) and tissue distribution was moderate (7 $L.kg^{-1}$), resulting in a long half-life (8.5 h). When dosed orally, **55** was absorbed quickly (T_{max} of 1 h) with a relatively good bioavailability (39%) (Table 7) (Supporting Information Figures S1 & S2). Oral absorption was likely limited by low aqueous solubility (5 μM) and moderate permeability (efflux ratio of 2.9 in Caco-2 cells) (Supporting Information Table S2). A 10% free fraction was determined for human plasma protein binding and was used as surrogate for mouse plasma protein binding towards determining free drug levels in vivo. (Supporting Information Figures S3). As compound **55** showed potent in vitro antiplasmodial activity and good DMPK properties, it was progressed to efficacy studies.

In vivo efficacy studies. Compound **55** was assessed for in vivo efficacy using the NSG mouse model of *P. falciparum* infection (*Pf*3D7 IC_{50} = 142 nM). NSG mice are genetically immunodeficient and thereby able to support engraftment by human red blood cells and infection by the human specific *P. falciparum* parasite.[24] A quadruple-dose regimen of 50 $mg.kg^{-1}$ of **55** for four consecutive days showed 80% reduction in parasitemia compared to untreated mice (Figure 3). The pharmacokinetics of **55** from the study showed good exposure and a dose-dependent correlation with the reduction in parasitemia (Table 8 and Figure 4). However, **55** had relatively slow killing kinetics (see below) and was cleared quickly. This likely accounts for parasitemia remaining flat throughout the course of the experiment.

Mechanism of action studies. The original hit compound **8** was disclosed in an oncology directed patent for compounds that act through inhibition of phosphatidylinositol-3-kinase (PI3K),[25] and assessment against *Plasmodium* lipid kinases showed it to be an inhibitor of PI4K from *P. vivax* with an IC_{50} of 1.9 μM. To support the inhibition of PI4K as the mode-of-action of the series, structurally diverse compounds, **21** and **26** were assessed against a panel

of six mechanistically distinct laboratory generated drug resistant strains of *P. falciparum*: *PfeEF2*, *Pfdxr*, *Pfpi4k*, *Pfdhodh*, *Pfcarl*, *PfcytB*.[10,26-29] Reduced susceptibility (2- and 3-fold, respectively) was only seen with the *Pfpi4k* mutant strain in line with the 5-fold reduced susceptibility of the strain for MMV390048 (Supporting Information Table S6) and in line with the PI4K mode-of-action.[10]

Plasmodium vivax PI4K enzyme assay. Compounds **21** and **26** showed potent inhibition (IC_{50} of 5 and 15 nM, respectively, Figure 5) of *Pv*PI4K, the only *Plasmodium* PI4K that has been isolated for enzymology work.[9,10] The catalytic domain of PI4KIIIβ in *P. falciparum* and *P. vivax* are well conserved and share 97% similarity; hence, the *Pv*PI4k is thought to be an adequate surrogate for expression of activity against *P. falciparum*. The clinical *Pf*PI4K inhibitor MMV390048 showed an IC_{50} of 3.4 nM in the *Pv*PI4K assay and 28 nM against *Pf*NF54.[10] This data supports inhibition of *Pf*PI4K as the antimalarial mode-of-action for the series though there is not a direct correlation between inhibitory potencies and antiplasmodial activity. Compound permeability through the host red blood cell and the parasite necessarily plays a role for expression of whole-cell activity.[30]

Parasite reduction ratio assay. Clearing the parasite quickly from the host system is deemed to be ideal to overcome mutations within the parasite and to mitigate resistance development. The IC_{50} of **30** against *Pf*3D7, the strain used in the parasite reduction ratio (PRR) assay, was 46 nM correlating closely to the value of 22 nM against NF54. The PRR experiment was run over 48 h showing a log PRR of **30** = 0.8 at a concentration of 10-fold over the IC_{50}, categorising the compound as also slow acting (Figure 6). *Pf*PI4K inhibitors have been previously reported to be moderately slow acting in the in vitro PRR assay and similar to atovaquone.[10] Hence the data is consistent in that the PI4K mode-of-action is associated with slower killing kinetics in the in vitro PRR assay.

Stage-specificity assay. The stage-specificity assay was performed using synchronous cultures of the drug sensitive NF54 strain to assess concentration-dependant growth response of rings and schizonts in the presence of compounds.[31] Compound **30** acted mostly on the later intra-erythrocytic schizonts stage of the parasite and showed little effect on the early ring stage. This correlates with the slow acting profile in the PRR assay and is comparable to the profile of MMV390048 (Figure 7).[10]

Computer Aided Drug Design (CADD) studies

Since compounds **21** and **26** showed potent PI4K inhibition, we investigated the putative receptor-ligand interactions in a homology model of *Pf*PI4K. The crystal structure of any plasmodium PI4K is unavailable at present, and so the X-ray crystal structure of human PI4KIIIβ (PDBID:4D0L) was used as a template[32] and the P*f*PI4K homology model was built using Schrodinger's PRIME protein modelling tool.[33] Docking studies revealed that **26** sits quite deep in the binding pocket (Figure 8) and delineated five interactions including four hydrogen bond interactions and one hydrophobic π-π stacking interaction. The naphthyridine 5-position nitrogen displayed a hydrogen bond with the backbone N-H of hinge residue Val1357 (Figure 9). The pyridine nitrogen of **26** formed a hydrogen bond with catalytic Lys1308. This interaction can account for the improvement in activity of **16** (NF54 IC_{50} = 122 nM) compared to the phenyl matched pair **10** (NF54 IC_{50} = 719 nM). The oxygen atoms in the sulfonamide group plausibly interacted with Ser1362 and Lys825. The residues highlighted in Figure 9, and others in the binding site, are strictly conserved in *P. vivax*, the isozyme which was used for enzyme inhibition studies. To support this model, the activities of **16** and **37** could be compared, where, replacement of sulfonamide in **16** with carboxamide in **37** (NF54 IC_{50} = 745 nM) resulted in a decrease in antiplasmodial activity. A face-to-face π-π stacking of the aryl ring at the naphthyridine 2-position with Phe827 was also observed.

As per the SAR interpretation, this interaction seems quite significant, as removal of the phenyl ring from **26** (NF54 IC_{50} = 87 nM) to afford **27** (NF54 IC_{50} >5000 nM) resulted in complete loss in activity**.** In summary, potential interactions envisaged using the P*f*PI4K homology model appear to be consistent with the SAR Both the methylsulfonyl and pyridyl groups of **26** extends towards solvent by this model suggesting further room for analogue modification, which might address physicochemical properties, pharmacokinetics and target potency.

CONCLUSION

Starting from an open source hit compound, MMV024101 (compound **8**) from the MMV Pathogen Box, a series of 2,8-disubstituted-1,5-naphthyridine analogues was synthesized and evaluated for in vitro antiplasmodial activity. From a total of 48 analogues made for SAR investigation, 26 showed improved blood stage activity compared to the original hit. Several analogues exhibited low nanomolar activity (NF54 IC_{50}'s <100 nM) and were equipotent against both NF54 and K1. Two compounds, **21** and **26**, were cross-resistant with a *Pfpi4k* laboratory mutant strain pointing to PI4K as the mode-of-action. The compounds were confirmed as potent inhibitors of *Pv*PI4K using a biochemical assay. The realization that the compounds operate on PI4K is significant in that the importance of the target is magnified by MMV390048 now in Phase IIa clinical trials. Major routes of metabolism of the 2- and 8-substituents of the naphthyridine ring were blocked *en route* to delivering the lead compound **55**. Compound **55** showed improved bioavailability in the mouse, and was chosen for in vivo efficacy studies based on the pharmacokinetics and antiplasmodial activity. In the *Pf*SCID mouse model of infection, **55** resulted in 80% reduction in parasitemia at 4 × 50 $mg.kg^{-1}$. At this juncture it is noteworthy that this compound meets the MMV Late Lead criteria with respect to CYP inhibition (IC_{50} >20 μM), oral bioavailability (>30%) and hERG (>10 μM)

but does not meet the in vitro antiplasmodial potency (IC_{50} <10 nM) criteria. By contrast, MMV390048 shows much higher efficacy with a similar reduction in parasitemia at 4 × 1 $mg.kg^{-1}$ and achieved 100% reduction in parasitemia at higher doses. This is a consequence of the much better pharmacokinetic profile and higher asexual blood stage activity of MMV390048.[10] Future optimization studies will aim to further improve pharmacokinetics and in vivo potency to enhance efficacy and to achieve the complete clearance of the malaria parasite that is comparable to other *Pf*PI4K inhibitors in development.

EXPERIMENTAL SECTION

All commercially available chemicals were purchased from either Sigma-Aldrich or Combi-Blocks. Unless otherwise stated, all solvents used were anhydrous. ^{1}H NMR spectra were recorded on a Bruker Spectrometer at 300 MHz. ^{13}C NMR were recorded either on a Bruker spectrometer at 400 MHz (^{1}H 400.2 MHz and ^{13}C 100.6 MHz) or Bruker-600 (^{1}H 600.3 MHz, ^{13}C 150.9 MHz). Analytical thin-layer chromatography (TLC) was performed on aluminum-backed silica-gel 60 F_{254} (70-230 mesh) plates. Column chromatography was performed with Merck silica-gel 60 (70-230 mesh). Chemical shifts (δ) are given in parts per million (ppm) downfield from TMS as the internal standard. Coupling constants, *J*, are recorded in Hertz (Hz). Standard acronyms representing multiplicity are used as follows: br s = broad singlet, s = singlet, d = doublet, t = triplet, m = multiplet. Purity was determined by Agilent 1260 Infinity binary pump, Agilent 1260 Infinity diode array detector (DAD), Agilent 1290 Infinity column compartment, Agilent 1260 Infinity standard autosampler, and Agilent 6120 quadrupole (single) mass spectrometer, equipped with APCI and ESI multimode ionization source and all compounds tested for biological activity were confirmed to have ≥95% purity. The HPLC method used is described in the Supporting Information.

Synthesis of 5-(((6-methoxypyridin-3-yl)amino)methylene)-2,2-dimethyl-1,3-dioxane-4,6-dione (2). A mixture of 2,2-dimethyl-1,3-dioxane-4,6-dione (29 g, 0.2 mol) and trimethoxymethane (198 mL, 1.8 mol) in ethanol (60 mL) was heated to 105 °C for 2 hours. 6-methoxypyridin-3-amine **1** (25 g, 0.2 mol) was then added and the resulting solution stirred at 105 °C for an additional 12 hours. The reaction mixture was allowed to cool to room temperature and diluted with hexane (200 mL). The precipitate was filtered and washed with hexane to afford 5-(((6-methoxypyridin-3-yl)amino)methylene)-2,2-dimethyl-1,3-dioxane-4,6-dione in 80% yield as a pale yellow solid. ^{1}H NMR (300 MHz, $CDCl_3$) δ = 11.18 (d, 1H, J = 13.8 Hz), 8.49 (d, 1H, J = 13.8 Hz), 8.13 (d, 1H, J = 2.8 Hz), 7.53 (dd, 1H, J = 8.9 Hz & 2.9 Hz), 6.83 (d, 1H, J = 8.9 Hz), 1.76 (s, 6 H), 3.97 (s, 3 H); Anal. RP-HPLC t_R = molecular ion peak not observed.

Synthesis of 6-methoxy-1,5-naphthyridin-4(1H)-one (3). 5-(((6-methoxypyridin-3-yl)amino)methylene)-2,2-dimethyl-1,3-dioxane-4,6-dione **2** (7.4 g, 26.6 mmol) was added portion wise to a preheated solution of Dowtherm A at 220 °C. After bubbling stopped, the mixture was allowed to cool to room temperature. The mixture was diluted with hexane, the precipitate was isolated, washed with hexane and dried to afford 6-methoxy-1,5-naphthyridin-4(1H)-one **3**, in 64% yield as a brown solid. ^{1}H NMR (300 MHz, DMSO-d_6) δ = 11.82 (br s, 1H), 7.95 (d, J = 8.3 Hz, 2H), 7.16 (d, J = 9.0 Hz, 1H), 6.23 (s, 1H), 3.93 (s, 3H); Anal. RP-HPLC t_R = 0.804 min (method 1, purity 99%); LC-MS APCI: m/z 177.1 $[M+H]^+$ (anal. calcd for $C_9H_8N_2O_2^+$: m/z = 176.1).

Synthesis of 8-bromo-2-methoxy-1,5-naphthyridine (4). Phosphorus tribromide (5 mL, 53.1 mmol) was added to a solution of 6-methoxy-1,5-naphthyridin-4(1-*H*)-one **3** (8.5 g, 48.2 mmol) in *N,N*-dimethylformamide (10 mL) at 0 °C. The mixture was continued to stir at 0 °C for 1 hour. The reaction mixture was diluted with deionized water (500 mL), and 6N NaOH

(1.3 mL) was added. The light brown precipitate was filtered off and thoroughly washed with deionized water. The resulting solid was taken up in ethyl acetate, and the solution was filtered through a pad of SiO_2 to afford 8-bromo-2-methoxy-1,5-naphthyridine **4**, in 87% yield as a pale brown solid. ^{1}H NMR (300 MHz, DMSO-d_6) δ = 8.36 (d, 1H, J = 4.8 Hz), 8.06 (d, 1H, J = 9.0 Hz), 7.83 (d, 1H, J = 4.8 Hz), 7.09 (d, 1H, J = 9.0 Hz), 3.83 (s, 3H); Anal. RP-HPLC t_R = 4.471 min (method 1, purity 98%); LC-MS APCI: *m/z* 239.0 $[M+H]^+$ (anal. calcd for $C_9H_7BrN_2O^+$: *m/z* = 238.0).

General procedure 1 for synthesis of intermediate 6 (GP1).

Synthesis of 8-(pyridin-4-yl)-1,5-naphthyridin-2-ol. A 25 mL round bottom flask was loaded with 2-methoxy-8-(pyridin-4-yl)-1,5-naphthyridine (0.91 g, 3.84 mmol) followed by dropwise addition of HBr (4.17 mL, 77 mmol) at room temperature. The resulting reaction mixture was heated at 85 °C for 12 hours. Excess of hydrogen bromide was evaporated from the reaction mixture *in vacuo*. The resulting residue was dissolved in 20 mL of dichloromethane/methanol 9:1 and loaded with Amberlyst 21. The resulting suspension was left to stir for 1 hour and filtered. The filtrate was evaporated *in vacuo* to afford 8-(pyridin-4-yl)-1,5-naphthyridin-2-ol in 94 % yield as white solid. ^{1}H NMR (300 MHz, DMSO-d_6) δ = 10.99 (br s, 1H), 8.79 – 8.72 (m, 2H), 8.58 (d, J = 4.7 Hz, 1H), 8.03 (d, J = 9.7 Hz, 1H), 7.65 – 7.57 (m, 2H), 7.47 (d, J = 4.7 Hz, 1H), 6.83 (d, J = 9.7 Hz, 1H); Anal. RP-HPLC t_R = 1.475 min (method 1, purity 99%); LC-MS APCI: *m/z* 224.1 $[M+H]^+$ (anal. calcd for $C_{13}H_9N_3O^+$: *m/z* = 223.1).

General procedure 2 for synthesis of intermediate 7 (GP2).

Synthesis of 2-bromo-8-(pyridin-4-yl)-1,5-naphthyridine. To a dry 25 ml round bottom flask, 8-(pyridin-4-yl)-1,5-naphthyridin-2-ol (0.3 g, 1.34 mmol) and phosphorus oxybromide

(1.16 g, 4.03 mmol) were added and stirred under inert atmosphere at 60 °C for 10 minutes. When the resulting reaction mixture liquefied, the temperature was increased to 120 °C and continued to stir for 2 hours. The resulting residue was dissolved in ethyl acetate (30 mL) and washed with deionized water (3 x 5 mL), dried over $MgSO_4$ and concentrated *in vacuo* to give 2-bromo-8-(pyridin-4-yl)-1,5-naphthyridine in 80% yield as a light brown powder. ^{1}H NMR (300 MHz, MeOD-d_4) δ = 9.08 (d, 1H, J = 4.5 Hz), 8.74-8.67 (m, 2H), 8.35 (d, 1H, J = 8.8 Hz), 7.96-7.89 (m, 2H), 7.87-7.83 (m, 2H); Anal. RP-HPLC t_R = 3.927 min (method 1, purity 98%); LC-MS APCI: *m/z* 286.0 $[M+H]^+$ (anal. calcd for $C_{13}H_8BrN_3^+$: *m/z* = 285.0).

General procedure 3 for nucleophilic substitution reaction (GP3).

Synthesis of N-(8-(pyridin-4-yl)-1,5-naphthyridin-2-yl)methanesulfonamide (27). To a solution of 2-bromo-8-(pyridin-4-yl)-1,5-naphthyridine (0.05 g, 0.18 mmol) in *N,N*-dimethylformamide (1.5 mL), methanesulfonamide (0.066 g, 0.699 mmol) and caesium carbonate (0.17 g, 0.52 mmol) were added into a 5 mL sealed tube. The resulting reaction mixture was heated at 110 °C and stirred for 12 hours. *N,N*-dimethylformamide was azeotropically evaporated from the reaction mixture *in vacuo* with the help of toluene. The residue was subjected to column chromatography on silica gel using hexane/ethyl acetate 5:5 v/v ratio initially and slowly increased to ethyl acetate/methanol 9:1 v/v ratio to elute N-(8-(pyridin-4-yl)-1,5-naphthyridin-2-yl)methanesulfonamide **27**, in 30% yield as a yellow solid. ^{1}H NMR (300 MHz, MeOD-d_4) δ = 8.92 (d, J = 4.6 Hz, 1H), 8.81 – 8.64 (m, 2H), 8.39 (d, J = 9.1 Hz, 1H), 8.07 – 7.97 (m, 2H), 7.88 (d, J = 4.6 Hz, 1H), 7.35 (d, J = 9.1 Hz, 1H), 3.17 (s, 3H). ^{13}C NMR (151 MHz, DMSO-d_6) δ = 152.07, 149.83, 149.14, 144.06, 142.26, 141.88, 140.54, 139.23, 125.54, 124.81, 117.28, 41.81; Anal. RP-HPLC t_R = 2.309 min (method 1, purity 99%); LC-MS APCI: *m/z* = 301.1 $[M+H]^+$ (anal. calcd for $C_{14}H_{12}N_4O_2S^+$: *m/z* = 300.1).

General procedure 4 for Buchwald-Hartwig cross-coupling reaction (GP4).

Synthesis of N-(3-(methylsulfonyl)phenyl)-8-(pyridin-4-yl)-1,5-naphthyridin-2-amine (28). $Pd_2(dba)_3$ (7.68 mg, 8.39 μmol) and dicyclohexyl(2',4',6'-triisopropyl-3,6-dimethoxy-[1,1'-biphenyl]-2-yl)phosphane (6.75 mg, 0.01 mmol) were dissolved in tert-butanol (1 mL) and toluene (1 mL) and stirred for 5 minutes. At which time 3-(methylsulfonyl)aniline (52.3 mg, 0.25 mmol) and caesium carbonate (96 mg, 0.29 mmol) were added. The reaction mixture was then heated at 115 °C for 12 hours. After concentration, the residue was subjected to column chromatography on silica gel using ethyl acetate to afford N-(3-(methylsulfonyl)phenyl)-8-(pyridin-4-yl)-1,5-naphthyridin-2-amine **28**, in 34% yield as pale yellow solid. ^{1}H NMR (300 MHz, DMSO-d_6) δ = 10.11 (br s, 1H), 8.78-8.75 (m, 3H), 8.51-8.47 (m, 1H), 8.52 (d, 1H, J = 9.1 Hz), 7.84 (t, 1H, J = 1.9 Hz), 7.77-7.75 (m, 2H), 7.68 (d, 1H, J = 4.5 Hz), 7.49-7.34 (m, 3H), 3.12 (s, 3H). ^{13}C NMR (101 MHz, DMSO-d_6) δ = 154.07, 149.88 (x 2), 147.20, 145.50, 142.24, 141.69, 141.61, 140.08, 139.16, 130.12, 125.25, 124.63, 123.36, 120.02, 118.47, 116.87, 44.08; Anal. RP-HPLC t_R = 0.312 min (method 2, purity 98%); LC-MS APCI: *m/z* 377.1 $[M+H]^+$ (anal. calcd for $C_{20}H_{16}N_4O_2S^+$: *m/z* = 376.1).

General procedure 5 for microwave mediated Suzuki cross-coupling reaction (GP5).

Synthesis of N-(2-hydroxyethyl)-3-(8-(pyridin-4-yl)-1,5-naphthyridin-2-yl)benzenesulfonamide (30). To a solution of 2-bromo-8-(pyridin-4-yl)-1,5-naphthyridine (0.200 g, 0.699 mmol) in Dioxane (5.5 mL) in 25mL microwave vial, (3-(N-(2-hydroxyethyl)sulfamoyl)phenyl)boronic acid (0.206 g, 0.839 mmol), $Pd_2(dba)_3$ (0.064 g, 0.070 mmol), tricyclohexylphosphane (0.047 g, 0.168 mmol) and Potassium phosphate

tribasic (0.445 g, 2.097 mmol) were added and degassed using N_2 for 5 minutes. Deionized water (1.38 mL) was then added and the reaction mixture was stirred for an additional 5 minutes. The mixture was microwaved in dynamic mode at 125 °C, 250 watts, 17.5 bar for 15 minutes. 1,4-Dioxane was removed under reduced pressure and the residue purified by column chromatography, hexane/ethyl acetate 5:5 v/v ratio initially and slowly increased to ethyl acetate/methanol 9.5:0.5 v/v ratio to elute N-(2-hydroxyethyl)-3-(8-(pyridin-4-yl)-1,5-naphthyridin-2-yl)benzenesulfonamide **30**, in 37% yield as yellow amorphous solid. ^{1}H NMR (300 MHz, DMSO-d_6) δ = 9.17 (d, 1H, J = 4.4 Hz), 8.89 (d, 2H, J = 5.3 Hz), 8.72-8.65 (m, 2H), 8.57 (d, 1H, J = 8.9 Hz), 8.51-8.44 (m, 1H), 8.13 (d, 2H, J = 5.3 Hz), 8.03 (d, 1H, J = 4.5 Hz), 7.93 (ddd, 1H, J = 7.8 Hz, 1.9 Hz & 1.1 Hz), 7.79 (t, 1H, J = 7.7 Hz), 7.69 (t, 1H, J = 5.9 Hz), 3.40 (t, 2H, J = 6.2 Hz), 2.86 (q, 2H, J = 6.1 Hz). ^{13}C NMR (151 MHz, DMSO-d_6) δ = 155.40, 152.12, 149.88, 144.57, 144.05, 143.73, 142.13, 140.42, 139.39, 139.17, 131.34, 130.53, 128.18, 125.85, 125.80, 125.13, 122.59, 60.40, 45.66; Anal. RP-HPLC t_R = 3.416 min (method 1, purity 99%); LC-MS APCI: m/z = 407.1 $[M+H]^+$ (anal. calcd for $C_{21}H_{18}N_4O_3S^+$: m/z = 406.1).

General procedure 6 for Suzuki cross-coupling reaction (GP6).

Synthesis of 3-(8-(2-(trifluoromethyl)pyridin-4-yl)-1,5-naphthyridin-2-yl)benzenesulfonamide (55). To a solution of 2-bromo-8-(2-(trifluoromethyl)pyridin-4-yl)-1,5-naphthyridine (0.300 g, 0.847 mmol) in 1,4-Dioxane (12.5 mL), 3-(4,4,5,5-tetramethyl-1,3,2-dioxaborolan-2-yl)benzenesulfonamide (0.264 g, 0.932 mmol), $PdCl_2$(dppf) (0.062 g, 0.085 mmol) and caesium carbonate (0.828 g, 2.54 mmol) were added, followed by deionized water (3.13 mL) in a 25 mL round bottom flask. The resulting reaction mixture was heated at 95 °C for 12 hours. 1,4-Dioxane was evaporated from the reaction mixture *in vacuo*. The resulting residue was dissolved in ethyl acetate (50 mL) and washed with water (3 x 15 mL),

dried over $MgSO_4$ and concentrated *in vacuo* to give a light brown solid. The residue was subjected to column chromatography on silica gel using hexane/ethyl acetate 8:2 v/v ratio initially and slowly increased to ethyl acetate/methanol 9:1 v/v ratio to elute 3-(8-(2-(trifluoromethyl)pyridin-4-yl)-1,5-naphthyridin-2-yl)benzenesulfonamide **55**, in 49% yield as white amorphous solid. ^{1}H NMR (300 MHz, MeOD-d_4) δ = 9.09 (d, 1H, J = 4.5 Hz), 8.94 (dt, 1H, J = 5.0 Hz & 0.7 Hz), 8.73 (td, 1H, J = 1.8 Hz & 0.5 Hz), 8.61 (d, 1H, J = 8.9 Hz), 8.46 (d, 1H, J = 8.9 Hz), 8.43-8.36 (m, 2H), 8.22 (dd, 1H, J = 5.1 Hz & 1.6 Hz), 8.04 (ddd, 1H, J = 7.9 Hz, 1.9 Hz & 1.1 Hz, 1H), 7.99 (d, 1H, J = 4.5 Hz), 7.69 (td, 1H, J = 7.8 Hz & 0.5 Hz). ^{13}C NMR (101 MHz, DMSO-d_6) δ = 155.78, 152.13, 150.50, 147.20, 146.22, 145.59, 143.74, 143.04, 140.18, 139.54, 138.89, 130.81, 130.23, 129.36, 127.57, 125.46, 124.94, 123.60, 122.71, 120.88; Anal. RP-HPLC t_R = 2.370 min (method 1, purity 98%); LC-MS APCI: *m/z* 431.0 $[M+H]^+$ (anal. calcd for $C_{20}H_{13}F_3N_4O_2S^+$: *m/z* = 430.1).

ASSOCIATED CONTENT

Supporting Information

Additional details of the characterization of selected compounds and the procedures used for the in vitro and in vivo antimalarial studies as well as PK and metabolism studies

SMILES nomenclature, NF54 and K1 IC_{50} values, biochemical and biological data (CSV)

AUTHOR INFORMATION

Corresponding Author

*Phone: +27-21-6502553. Fax: +27-21-6505195. E-mail: Kelly.Chibale@uct.ac.za

ORCID

Kelly Chibale: 0000-0002-1327-4727

Notes

The authors declare no competing financial interest.

ACKNOWLEGEMENTS

We thank the Merck Global Health Institute for financial support for this research. The University of Cape Town, South African Medical Research Council, and South African Research Chairs initiative of the Department of Science and Technology, administered through the South African National Research Foundation, are gratefully acknowledged for support (K.C.). We thank Paul. A. Willis and James Duffy of MMV for assistance with the Pathogen Box. We thank Laura Maria Sanz Alonso of GlaxoSmithKline for support with the PRR assay. We thank Sergio Wittlin and Christian Scheurer for support with the cross-resistance and stage-specificity assays. We thank John E. Burke of University of Victoria for the *Pv*PI4K enzyme assay as well as Anjo Theron and Dalu Mancama of the Council for Scientific and Industrial Research (South Africa) for gametocytocidal activity assays. We extend our thanks to Virgil Verhoog and Sumaya Salie for assistance in performing the antiplasmodial assays and Nesia Barnes, Warren Olifant and Duane Knowles for their assistance with the ADME assays. TS thanks his colleagues from Merck KGaA Darmstadt Germany for logistical support and for generating *h*ERG, Caco-2, and LogD data. We also thank the South African Western Province Blood Transfusion Services for donating human erythrocytes used in the study.

ABBREVIATIONS USED

WHO, world health organization; ACT, artemisinin-based combination therapy; PI4K, phosphatidylinositol-4-kinase; PI, phosphatidylinositol; PI4P, phosphatidylinositol-4-phosphate; MMV, medicines for malaria venture; PK, pharmacokinetics; ADME, absorption, distribution, metabolism, and excretion; SAR, structure-activity relationships; DMPK; drug metabolism and pharmacokinetics; ABT, 1-aminobenzotriazole; PRR, parasite reduction ratio; NMR, nuclear magnetic resonance; TMS, tetramethylsilane; TLC, thin-layer chromatography; HPLC, high pressure liquid chromatography; LC-MS, liquid chromatography-mass spectrometry

REFERENCES

1. *World Malaria Report* 2017; World Health Organization: Geneva, Switzerland, **2017**.

2. Phillips, M. A.; Burrows, J. N.; Manyando, C.; van Huijsduijnen, R. H.; Van Voorhis, W. C.; Wells, T. N. C. Malaria. *Nat. Rev. Dis. Prim.* **2017**, *3*, 17050, 1-24.

3. Blasco, B.; Leroy, D.; Fidock, D. A. Antimalarial Drug Resistance: Linking *Plasmodium falciparum* Parasite Biology to the Clinic. *Nat. Med.* **2017**, *23* (8), 917–928.

4. Dondorp, A. M.; Nosten, F.; Yi, P.; Das, D.; Phyo, A. P.; Tarning, J.; Lwin, K. M.; Ariey, F.; Hanpithakpong, W.; Lee, S. J.; Ringwald, P.; Silamut, K.; Imwong, M.; Chotivanich, K.; Lim, P.; Herdman, T.; An, S. S.; Yeung, S.; Singhsivanon, P.; Day, N. P.; Lingegardh, N.; Socheat, D.; White, N. J. Artemisinin Resistance in *Plasmodium falciparum* Malaria. *N. Engl. J. Med*. **2009**, *361*, 455−467.

5. Gamo, F.-J. Antimalarial Drug Resistance: New Treatments Options for *Plasmodium*. *Drug Discov. Today Technol.* **2014**, *11*, 81–88.

6. Hallyburton, I.; Grimaldi, R.; Woodland, A.; Baragaña, B.; Luksch, T.; Spinks, D.; James, D.; Leroy, D.; Waterson, D.; Fairlamb, A. H.; Wyatt, P. G.; Gilbert, I. H.; Frearson, J. A. Screening a Protein Kinase Inhibitor Library against *Plasmodium falciparum*. *Malar. J.* **2017**, *16* (1), 1–11.

7. Solyakov, L.; Halbert, J.; Alam, M. M.; Semblat, J.-P.; Dorin-Semblat, D.; Reininger, L.; Bottrill, A. R.; Mistry, S.; Abdi, A.; Fennell, C.; Holland, Z.; Demarta, C.; Bouza, Y.; Sicard, A.; Nivez, M.-P.; Eschenlauer, S.; Lama, T.; Thomas, D. C.; Sharma, P.; Agarwal, S.; Kern, S.; Pradel, G.; Graciotti, M.; Tobin, A. B.; Doerig, C. Global Kinomic and Phospho-Proteomic Analyses of the Human Malaria Parasite *Plasmodium falciparum*. *Nat. Commun.* **2011**, *2*, 565.

8. Balla, T. Phosphoinositides: Tiny Lipids With Giant Impact on Cell Regulation. *Physiol. Rev.* **2013**, *93* (3), 1019–1137.

9. McNamara, C. W.; Lee, M. C. S.; Lim, C. S.; Lim, S. H.; Roland, J.; Nagle, A.; Simon, O.; Yeung, B. K. S.; Chatterjee, A. K.; McCormack, S. L.; Manary, M. J.; Zeeman, A. M.; Dechering, K. J.; Kumar, T. R. S.; Henrich, P. P.; Gagaring, K.; Ibanez, M.; Kato, N.; Kuhen, K. L.; Fischli, C.; Rottmann, M.; Plouffe, D. M.; Bursulaya, B.; Meister, S.; Rameh, L.; Trappe, J.; Haasen, D.; Timmerman, M.; Sauerwein, R. W.; Suwanarusk, R.; Russell, B.; Renia, L.; Nosten, F.; Tully, D. C.; Kocken, C. H. M.; Glynne, R. J.; Bodenreider, C.; Fidock, D. A.; Diagana, T. T.; Winzeler, E. A. Targeting *Plasmodium* PI(4)K to Eliminate Malaria. *Nature* **2013**, *504* (7479), 248–253.

10. Paquet, T.; Le Manach, C.; Cabrera, D. G.; Younis, Y.; Henrich, P. P.; Abraham, T. S.; Lee, M. C. S.; Basak, R.; Ghidelli-Disse, S.; Lafuente-Monasterio, M. J.; Bantscheff, M.; Ruecker, A.; Blagborough, A. M.; Zakutansky, S. E.; Zeeman, A. M.;

White, K. L.; Shackleford, D. M.; Mannila, J.; Morizzi, J.; Scheurer, C.; Angulo-Barturen, I.; Santosmartínez, M.; Ferrer, S.; Sanz, L. M.; Gamo, F. J.; Reader, J.; Botha, M.; Dechering, K. J.; Sauerwein, R. W.; Tungtaeng, A.; Vanachayangkul, P.; Lim, C. S.; Burrows, J.; Witty, M. J.; Marsh, K. C.; Bodenreider, C.; Rochford, R.; Solapure, S. M.; Jiménez-Díaz, M. B.; Wittlin, S.; Charman, S. A.; Donini, C.; Campo, B.; Birkholtz, L. M.; Khanson, K.; Drewes, G.; Kocken, C. M.; Delves, M. J.; Leroy, D.; Fidock, D. A.; Waterson, D.; Street, L. J.; Chibale, K. Antimalarial Efficacy of MMV390048, an Inhibitor of *Plasmodium* Phosphatidylinositol 4-Kinase. *Sci. Transl. Med.* **2017**, *9* (387), 1-14.

11. ClinicalTrials.gov. (2018). MMV390048 POC in Patients With *P. vivax* and *P. falciparum* Malaria. [online] Available at: https://clinicaltrials.gov/ct2/show/NCT02880241 [Accessed 26 Mar. 2018].

12. Kato, N.; Comer, E.; Sakata-Kato, T.; Sharma, A.; Sharma, M.; Maetani, M.; Bastien, J.; Brancucci, N. M.; Bittker, J. A.; Corey, V.; Clarke, D.; Derbyshire, E. R.; Dornan, G. L.; Duffy, S.; Eckley, S.; Itoe, M. A.; Koolen, K. M. J.; Lewis, T. A.; Lui, P. S.; Lukens, A. K.; Lund, E.; March, S.; Meibalan, E.; Meier, B. C.; McPhail, J. A.; Mitasev, B.; Moss, E. L.; Sayes, M.; Van Gessel, Y.; Wawer, M. J.; Yoshinaga, T.; Zeeman, A. M.; Avery, V. M.; Bhatia, S. N.; Burke, J. E.; Catteruccia, F.; Clardy, J. C.; Clemons, P. A.; Dechering, K. J.; Duvall, J. R.; Foley, M. A.; Gusovsky, F.; Kocken, C. H. M.; Marti, M.; Morningstar, M. L.; Munoz, B.; Neafsey, D. E.; Sharma, A.; Winzeler, E. A.; Wirth, D. F.; Scherer, C. A.; Schreiber, S. L. Diversity-Oriented Synthesis Yields Novel Multistage Antimalarial Inhibitors. *Nature* **2016**, *538* (7625), 344–349.

13. Pathogenbox.org. (2018). The Pathogen Box | Catalysing Neglected Disease Drug Discovery. [online] Available at: https://www.pahogenbox.org/ [Accessed 4 Mar. 2018].

14. Gamo, F.-J.; Sanz, L. M.; Vidal, J.; de Cozar, C.; Alvarez, E.; Lavandera, J.-L.; Vanderwall, D. E.; Green, D. V. S.; Kumar, V.; Hasan, S.; Brown, J. R.; Peishoff, C. E.; Cardon, L. R.; Garcia-Bustos, J. F. Thousands of Chemical Starting Points for Antimalarial Lead Identification. *Nature* **2010**, *465* (7296), 305–310.

15. Spangenberg, T.; Burrows, J. N.; Kowalczyk, P.; McDonald, S.; Wells, T. N. C.; Willis, P. The Open Access Malaria Box: A Drug Discovery Catalyst for Neglected Diseases. *PLoS One* **2013**, *8* (6), e62906.

16. Duffy, S.; Sykes, M. L.; Jones, A. J.; Shelper, T. B.; Simpson, M.; Lang, R.; Poulsen, S.-A.; Sleebs, B. E.; Avery, V. M. Screening the MMV Pathogen Box across Multiple Pathogens Reclassifies Starting Points for Open Source Drug Discovery. *Antimicrob. Agents Chemother.* **2017**, *61* (9), AAC.00379-17.

17. Allison, B. D.; Gomez, L.; Grice, C. A.;.Hack, M. D.; Morrow, B. J.; Motley, T. S.; Santillan, A.; Shaw, K. J.; Schwarz, K. L.; Tang, L. Y.; Venkatesan, H.; Wiener, J. Preparation of Tetrahydroindazoles and Analogs as Inhibitors of DNA Gyrase and Topoisomerase IV for the Treatment of Bacterial Infection. WO/2006/0150289, October 5, 2006.

18. Miyaura, N.; Suzuki, A. Palladium-Catalyzed Cross-Coupling Reactions of Organoboron Compounds. *Chem. Rev*. **1995**, *95*, 2457− 2483.

19. Ishiyama, T.; Murata, M.; Miyaura, N. Palladium(0)-Catalyzed Cross-Coupling Reaction of Alkoxydiboron with Haloarenes: A Direct Procedure for Arylboronic Esters. *J. Org. Chem.* **1995**, *60* (23), 7508–7510.

20. Kerns, E. H.; Di, L. Drug-like Properties: Concepts, Structure, Design and Methods; Academic Press: San Diego, CA, 2008.

21. Nagib, D. A.; Macmillan, D. W. C. Trifluoromethylation of Arenes and Heteroarenes by Means of Photoredox Catalysis. *Nature* **2011**, *480* (7376), 224–228.

22. Watanabe, A.; Mayumi,K.; Nishimura, K.; Osaki, H. In Vivo use of the CYP Inhibitor 1-Aminobenzotriazole to Increase Long-term Exposure in Mice. *Biopharm. Drug Dispos.* **2016**, *37*, 373–378.

23. Linder, C. D.; Renaud, N. A.; Hutzler, J. M. Is Aminobenzotriazole an Appropriate in Vitro Tool as a Nonspecific Cytochrome P450 Inactivator? Drug Metab. Dispos. **2009**, *37*, 10–13.

24. Angulo-Barturen, I.; Jiménez-Díaz, M. B.; Mulet, T.; Rullas, J.; Herreros, E.; Ferrer, S.; Jiménez, E.; Mendoza, A.; Regadera, J.; Rosenthal, P. J.; Bathurst, I.; Pompliano, D. L.; de las Heras, F. G.; Gargallo-Viola, D. A Murine Model of *falciparum*-Malaria by in Vivo Selection of Competent Strains in Non-Myelodepleted Mice Engrafted with Human Erythrocytes. *PLoS One* **2008**, *3* (5), e2252.

25. Adams, N. D.; Burgess, J. L.; Chaudhari, A. M.; Knight, S. D.; Parrish, C. A. Naphthyridine Derivatives as PI3 Kinase Inhibitors. WO/2008/0150827, December 11, 2008.

26. Baragaña, B.; Hallyburton, I.; Lee, M. C. S.; Norcross, N. R.; Grimaldi, R.; Otto, T. D.; Proto, W. R.; Blagborough, A. M.; Meister, S.; Wirjanata, G.; Ruecker, A.; Upton, L. M.; Abraham, T. S.; Almeida, M. J.; Pradhan, A.; Porzelle, A.; Martínez, M. S.; Bolscher, J. M.; Woodland, A.; Norval, S.; Zuccotto, F.; Thomas, J.; Simeons, F.; Stojanovski, L.; Osuna-Cabello, M.; Brock, P. M.; Churcher, T. S.; Sala, K. A.; Zakutansky, S. E.; Jiménez-Díaz, M. B.; Sanz, L. M.; Riley, J.; Basak, R.; Campbell, M.; Avery, V. M.; Sauerwein, R. W.; Dechering, K. J.; Noviyanti, R.; Campo, B.;

Frearson, J. A.; Angulo-Barturen, I.; Ferrer-Bazaga, S.; Gamo, F. J.; Wyatt, P. G.; Leroy, D.; Siegl, P.; Delves, M. J.; Kyle, D. E.; Wittlin, S.; Marfurt, J.; Price, R. N.; Sinden, R. E.; Winzeler, E. A.; Charman, S. A.; Bebrevska, L.; Gray, D. W.; Campbell, S.; Fairlamb, A. H.; Willis, P. A.; Rayner, J. C.; Fidock, D. A.; Read, K. D.; Gilbert, I. H. A Novel Multiple-Stage Antimalarial Agent That Inhibits Protein Synthesis. *Nature* **2015**, *522* (7556), 315–320.

27. Dharia, N. V.; Sidhu, A. B. S.; Cassera, M. B.; Westenberger, S. J.; Bopp, S. E. R.; Eastman, R. T.; Plouffe, D.; Batalov, S.; Park, D. J.; Volkman, S. K.; Wirth, D. F.; Zhou, Y.; Fidock, D. A.; Winzeler, E. A. Use of High-Density Tiling Microarrays to Identify Mutations Globally and Elucidate Mechanisms of Drug Resistance in *Plasmodium falciparum*. *Genome Biol.* **2009**, *10* (2), R21.

28. Meister, S.; Plouffe, D. M.; Kuhen, K. L.; Bonamy, G. M. C.; Wu, T.; Barnes, S. W.; Bopp, S. E.; Borboa, R.; Bright, A. T.; Che, J.; Cohen, S.; Dharia, N. V; Gagaring, K.; Gettayacamin, M.; Gordon, P.; Groessl, T.; Kato, N.; Lee, M. C. S.; Mcnamara, C. W.; Fidock, D. A.; Nagle A.; Nam T. G.; Richmond W.; Roland J.; Rottmann M.; Zhou B.; Froissard P.; Glynne R. J.; Mazier D.; Sattabongkot J.; Schultz P. G.; Tuntland T.; Walker J. R.; Zhou Y.; Chatterjee A.; Diagana T. T.; Winzeler E. A. Imaging of *Plasmodium* Liver Stages to Drive Next-generation Antimalarial Drug Discovery. *Science* **2011**, *334*, 1372–1377.

29. Stickles, A. M.; De Almeida, M. J.; Morrisey, J. M.; Sheridan, K. A.; Forquer, I. P.; Nilsen, A.; Winter, R. W.; Burrows, J. N.; Fidock, D. A.; Vaidya, A. B.; Riscoe, M. K. Subtle Changes in Endochin-like Quinolone Structure Alter the Site of Inhibition within the Cytochrome bc_1 Complex of *Plasmodium falciparum*. *Antimicrob. Agents Chemother.* **2015**, *59* (4), 1977–1982.

30. Basore, K.; Cheng, Y.; Kushwaha, A. K.; Nguyen, S. T.; Desai, S. A. How Do Antimalarial Drugs Reach Their Intracellular Targets? *Front. Pharmacol.* **2015**, *6* (MAY), 1–7.

31. Le Manach, C.; Scheurer, C.; Sax, S.; Schleiferböck, S.; Cabrera, D. G.; Younis, Y.; Paquet, T.; Street, L.; Smith, P.; Ding, X. C.; Waterson, D.; Witty, M. J.; Leroy, D.; Chibale, K.; Wittlin, S. Fast in Vitro Methods to Determine the Speed of Action and the Stage-Specificity of Anti-Malarials in *Plasmodium falciparum*. *Malar. J.* **2013**, *12* (1), 1–7.

32. Burke, J. E.; Inglis, A. J.; Perisic, O.; Masson, G. R.; McLaughlin, S. H.; Rutaganira, F.; Shokat, K. M.; Williams, R. L. Structures of PI4KIIIβ Complexes Show Simultaneous Recruitment of Rab11 and Its Effectors. *Science* **2014**, *344 (6187)*, 1035-1038.

33. Schrodinger Release **2014-**1, Schrodinger, Inc.: 2014.

34. Singh, K.; Okombo, J.; Brunschwig, C.; Ndubi, F.; Barnard, L.; Wilkinson, C.; Njogu, P. M.; Njoroge, M.; Laing, L.; Machado, M.; Prudêncio, M.; Reader, J.; Botha, M.; Nondaba, S.; Birkholtz, L. M.; Lauterbach, S.; Churchyard, A.; Coetzer, T. L.; Burrows, J. N.; Yeates, C.; Denti, P.; Wiesner, L.; Egan, T. J.; Wittlin, S.; Chibale, K. Antimalarial Pyrido[1,2-A]benzimidazoles: Lead Optimization, Parasite Life Cycle Stage Profile, Mechanistic Evaluation, Killing Kinetics, and in Vivo Oral Efficacy in a Mouse Model. *J. Med. Chem.* **2017**, *60* (4), 1432–1448.

TABLE OF CONTENTS GRAPHIC

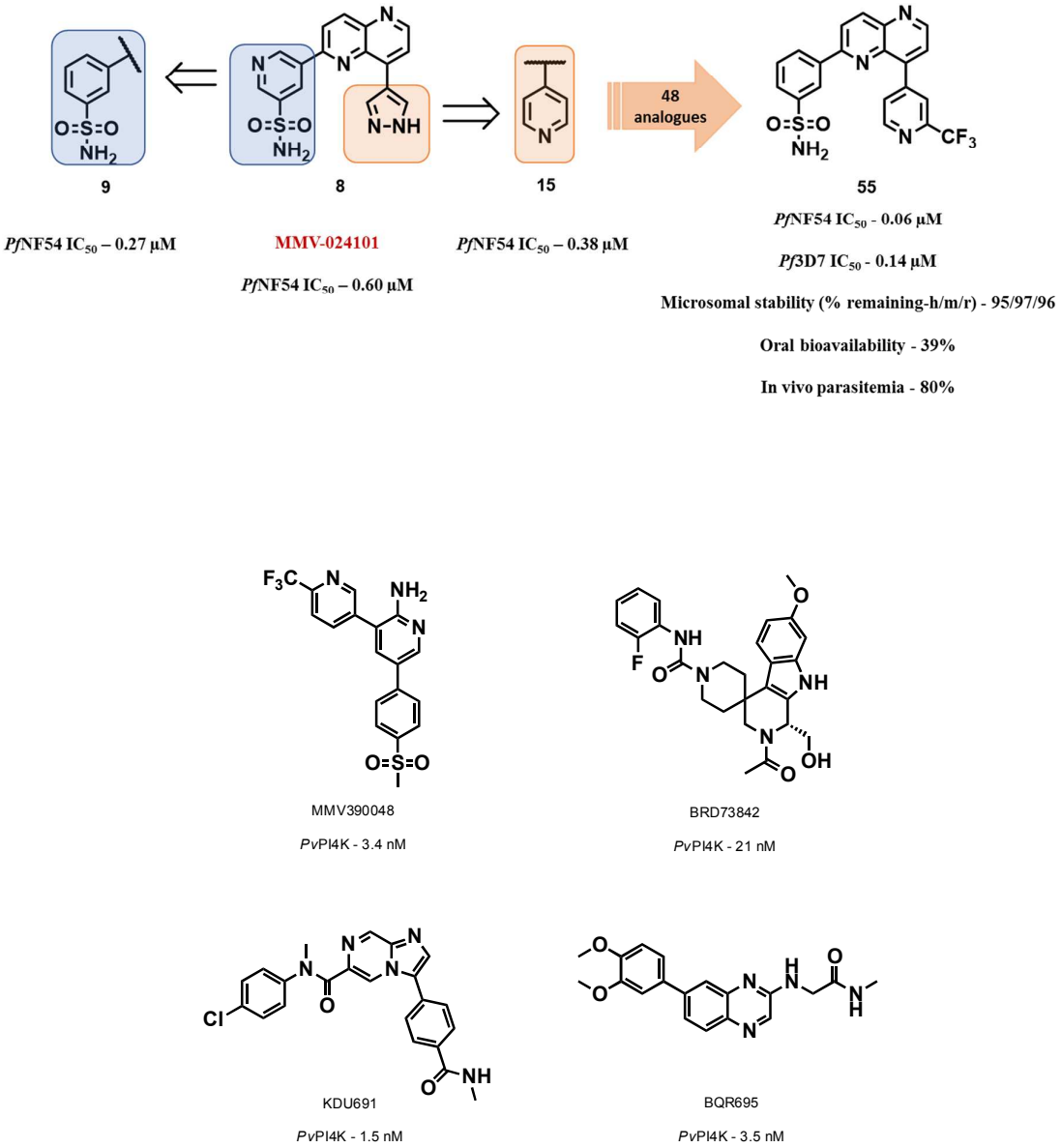

Figure 1: Antiplasmodial agents targeting *Pf*PI4-kinases.

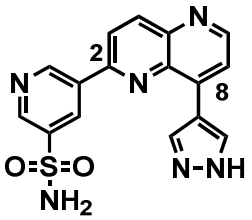

MMV024101

Compound 8

Figure 2: Structure of MMV024101

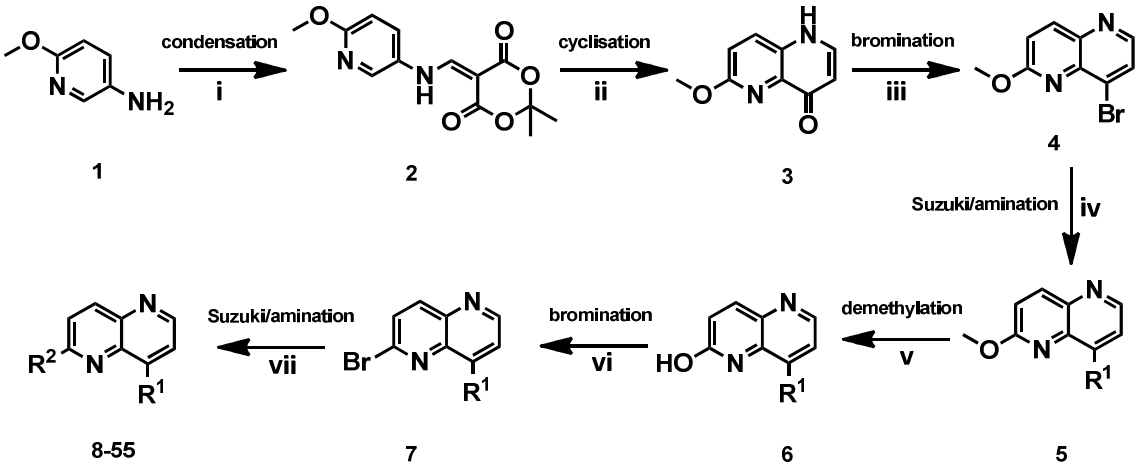

Scheme 1: Synthesis of 2,8-disubstituted 1,5-naphthyridines[a]

[a]Reagents and conditions: (i) 2,2-dimethyl-1,3-dioxane-4,6-dione, trimethoxymethane, ethanol, 105 ºC, 12 h, 80%; (ii) Dowtherm A, 220 ºC, 64%; (iii) PBr_3, DMF, 0 ºC to rt, 87%; (iv) R^1-$B(OH)_2$, $PdCl_2$(dppf), Cs_2CO_3, dioxane, 95 ºC, 41%-91%; or R^1-appropriate amine, Cs_2CO_3, DMF, 110 ºC, 12 h, 45%-71%; (v) HBr, 85 ºC, 89%-95%; (vi) $POBr_3$, 60 ºC to 120 ºC, 55%-91%; (vii) R^2-$B(OH)_2$, $PdCl_2$(dppf), Cs_2CO_3, dioxane, 95 ºC, 8-64%; or R^2-$B(OH)_2$, $Pd_2(dba)_3$, PCy_3, K_3PO_4, dioxane, 125 ºC, 17-23%; or R^2-appropriate amine, Cs_2CO_3, DMF, 110 ºC, 12 h, 30-41%; or R^2-appropriate aromatic amine, $Pd_2(dba)_3$, BrettPhos, Cs_2CO_3, toluene, tert-butanol, 115 ºC, 34%.

Table 1: Antiplasmodium activity and water solubility for analogues based on the hit compound **8**

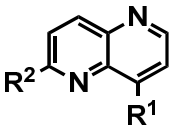

Compd	R^1	R^2	[a]Pf IC_{50} (nM)		[b]Aqueous solubility (μM) pH-6.5
			NF54	K1	
	Chloroquine[c]		16	194	
	Artesunate[c]		4	3	
8		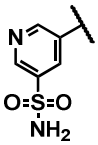	543	-	<5
9		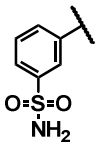	277	215	<5
10		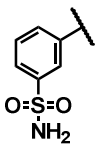	719	-	-

11	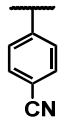	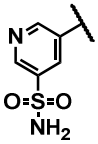	424	-	-
12	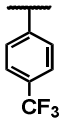	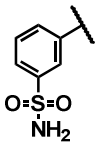	265	-	-
13	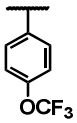	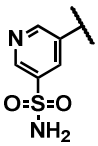	355	-	-
14	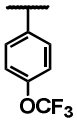	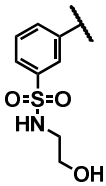	457	412	<5
15		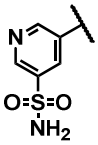	377	284	-
16		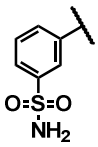	122	-	<5
17		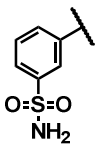	119	238	<5

18	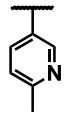	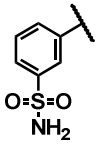	84	-	<5
19		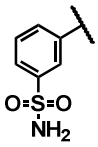	91	105	<5
20	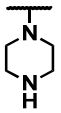	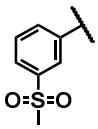	910	-	165
21	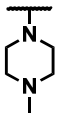	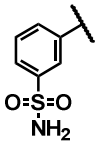	727	437	200
22	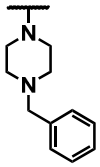	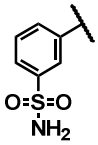	728	-	<5

[a]Mean from n values of ≥2 independent experiments. [b]Kinetic aqueous solubility using HPLC-DAD-MS. [c]Data from Singh, K et al.[34]

Table 2: Modifications at the 2-position of the 1,5-naphthyridine ring

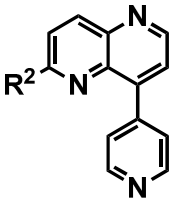

Compd	R^2	[a]Pf IC_{50} (nM)		[b]Aqueous solubility	[c]Cytotoxicity		[d]Metabolic stability
		NF54	K1	(μM) pH-6.5	CHO IC_{50} (µM)	SI	(% remaining after 30 min) (h/m/r)
Emetine[e]					0.095		
16	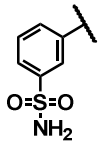	122	-	<5	2	16	-
23	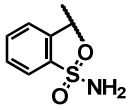	>5000	-	<5	-	-	-
24	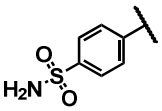	>5000	-	25	-	-	76/13/36
25	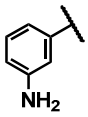	935	-	<5	-	-	78/54/61

26	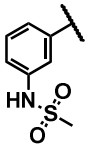	87	110	20	13	253	59/50/49
27		>5000	-	90	-	-	96/95/94
28	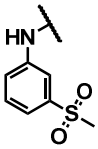	496	-	-	>50	>1000	-
29	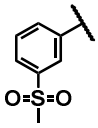	147	-	<5	13	85	-
30	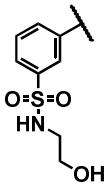	22	19	115	4	184	59/38/58
31	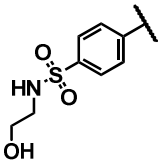	6180	-	50	-	-	-

32	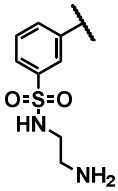	708	-	200	-	-	-
33	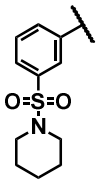	1432	-	15	-	-	-
34	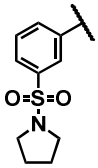	1484	-	<5	-	-	-
35	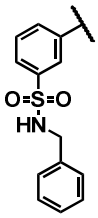	31	65	<5	>50	>1000	42/2/6
36	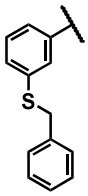	3668	-	-	-	-	-
37	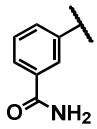	745	-	-	-	-	-

38	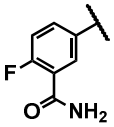	1755	-	-	-	-	-
39	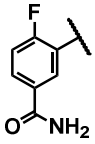	>5000	-	-	-	-	-
40	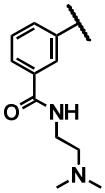	2623	-	-	-	-	-
41	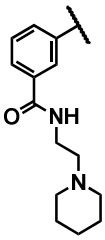	1360	-	-	-	-	-
42	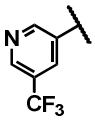	>1000	-	-	-	-	-
43	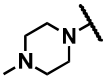	>1000	-	-	-	-	-
44		>1000	-	-	-	-	-

45		>1000	-	90	-	-	-

[a]Mean from n values of ≥2 independent experiments. [b]Kinetic aqueous solubility using HPLC-DAD-MS. [c]CHO = Chinese hamster ovarian cell line. SI is selectivity index = [IC_{50}(CHO)/IC_{50}(*Pf*NF54)]. [d]Human, mice, rat liver microsomes. [e]Data from Singh, K et al.[34]

Table 3: 1,5- Naphthyridine analogues based on Compound **30**

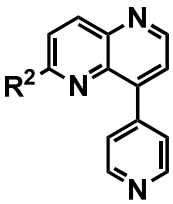

Compd	**R^2**	**[a]Pf IC_{50} (nM)**		**[b]Aqueous Solubility (μM) pH-6.5**	**[c]Cytotoxicity**		**[d]Metabolic stability (% remaining after 30 min) (h/m/r)**
		NF54	**K1**		**CHO IC_{50} (μM)**	**SI**	
30	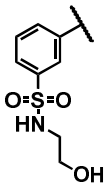	22	19	115	4	184	59/38/58

46	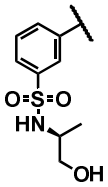	1015	-	50	-	-	-
47	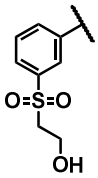	84	-	55	26	300	95/52/59
48	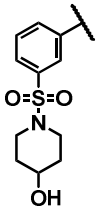	29	-	10	8	272	5/7/11
49	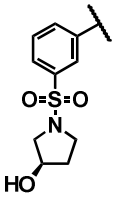	187	-	20	9	50	17/12/10
50	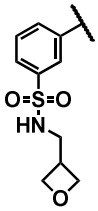	203	-	20	16	79	2/19/8

51	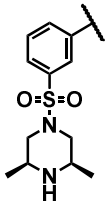	46	-	180	6	135	34/33/36
52	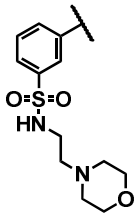	50	-	195	-	-	<1/<1/<1
53	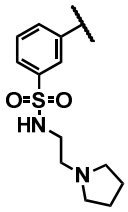	31	25	175	5	161	56/60/66

[a]Mean from n values of ≥2 independent experiments. [b]Kinetic aqueous solubility using HPLC-DAD-MS. [c]CHO = Chinese hamster ovarian cell line. SI is selectivity index = [IC_{50} (CHO)/IC_{50}(*Pf*NF54)]. [d]Human, mice, rat liver microsomes.

Table 4: 8-Trifluoromethylpyridine analogues

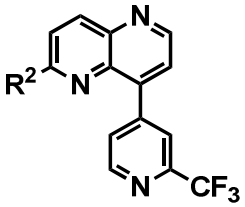

Compd	R^2	[a]Pf IC_{50} (nM)		[b]Aqueous solubility (μM) pH-6.5	[c]Cytotoxicity		[d]Metabolic stability (% remaining after 30 min) (h/m/r)
		NF54	K1		CHO IC_{50} (µM)	SI	
54	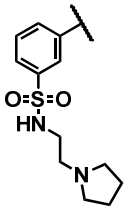	20	46	145	13	448	14/8/16
55	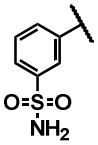	63	102	5	6	88	95/97/96

[a]Mean from n values of ≥2 independent experiments. [b]Kinetic aqueous solubility using HPLC-DAD-MS. [c]CHO = Chinese hamster ovarian cell line. SI is selectivity index = [IC_{50}(CHO)/IC_{50}(*Pf*NF54)]. [d]Human, mice, rat liver microsomes.

Table 5: In vitro CYP isoform inhibition

Compd	Cytochrome P450 inhibition (µM)			
	3A4	2C9	2D6	2C19

30	>20	>20	>20	>20

Table 6: In vitro hERG activity

Compd	**19**	**30**	**35**	**55**
hERG IC_{50} (μM)	>10	>10	1.2	>10

Table 7: Mouse pharmacokinetic parameters of compounds **30** and **55**

Parameter	30			16			55	
	iv	oral	oral with ABT	iv	oral	oral with ABT	iv	oral
Nominal dose (mg.kg^{-1})	2	20	20	2	20	20	1.5	5
C_{max} (μM)	-	0.5	0.5	-	5.0	0.5	-	2.8
T_{max} (h)	-	0.5	0.5	-	0.5	0.5-1	-	1
apparent $t_{1/2}$ (h)	3.3	3.3	4.5	2.5	1.6	3.2	8.5	33
CL (mL.min^{-1} kg^{-1})	89.5	-	-	-	-	-	11	-
V_d (L.kg^{-1})	25.7	-	-	-	-	-	7	-
$AUC_{0-\infty}$ (μM.min^{-1})	56	44	86	111	523	243	350	452
Oral bioavailability (%)	-	8	15	-	-	-	-	39

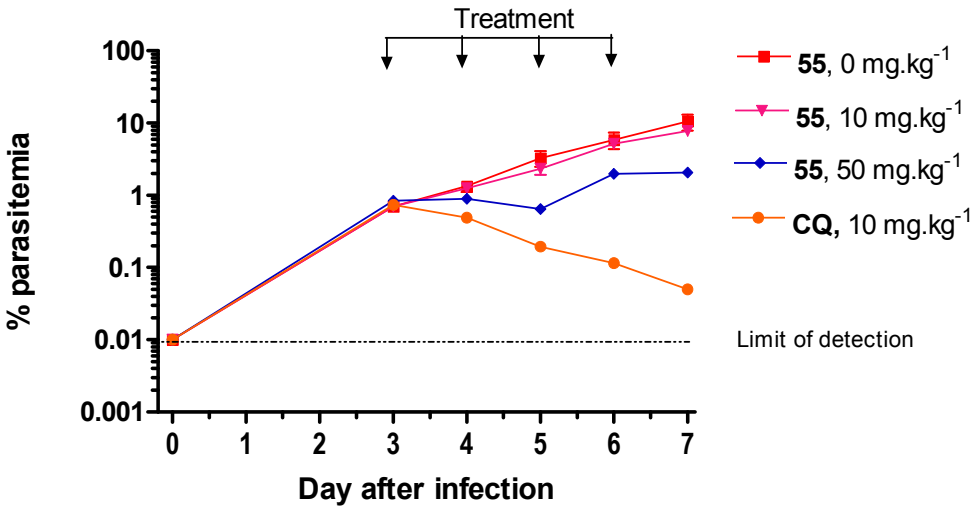

Figure 3: In vivo efficacy of **55** in the NOD-scid mouse model (n=2)

Table 8: Mean pharmacokinetic parameters of Compound 55 from po dosing in the NOD-scid mouse model

Parameter	**Mean dose (mg.kg^{-1})**			
	50	10	5	2.5
C_{max} (μM)	6.36	2.23	1.47	0.75
T_{max} (h)	2.5	4	4	4
AUC $_{0\text{-}24}$ (μM.min^{-1})	5591	2035	1198	658

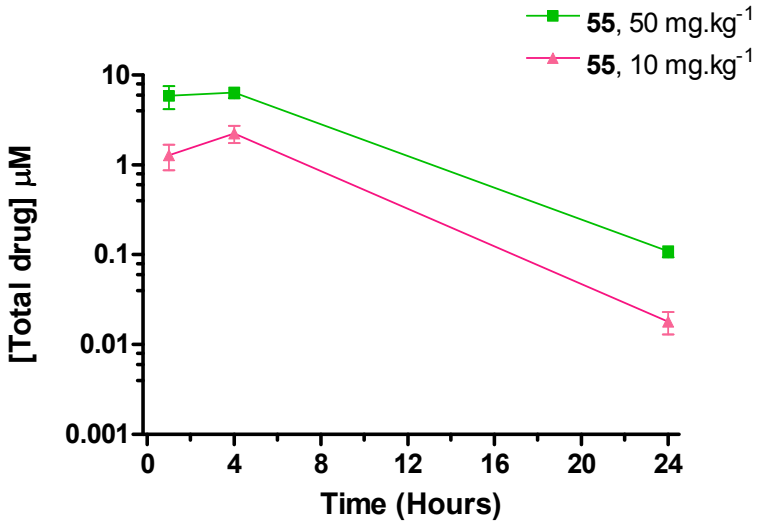

Figure 4: Plasma concentrations of 55 following po dosing in the NOD-scid mouse model

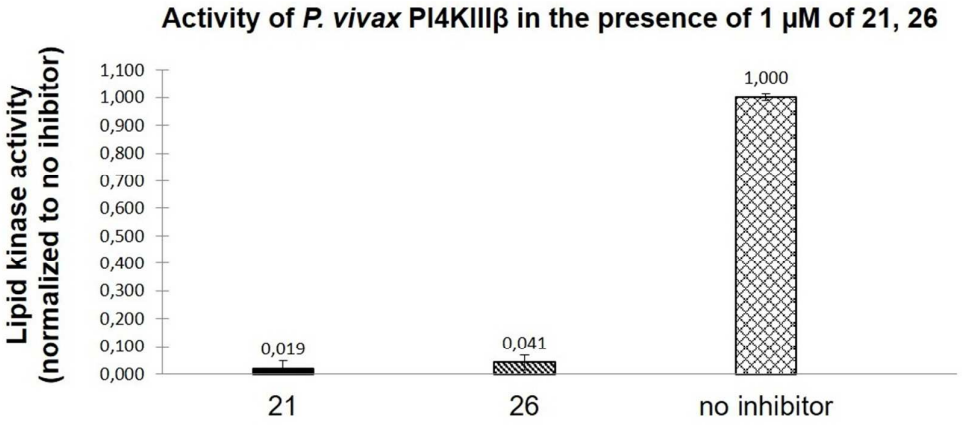

Figure 5: Inhibition of *Pv*PI4K by compounds **21** and **26**

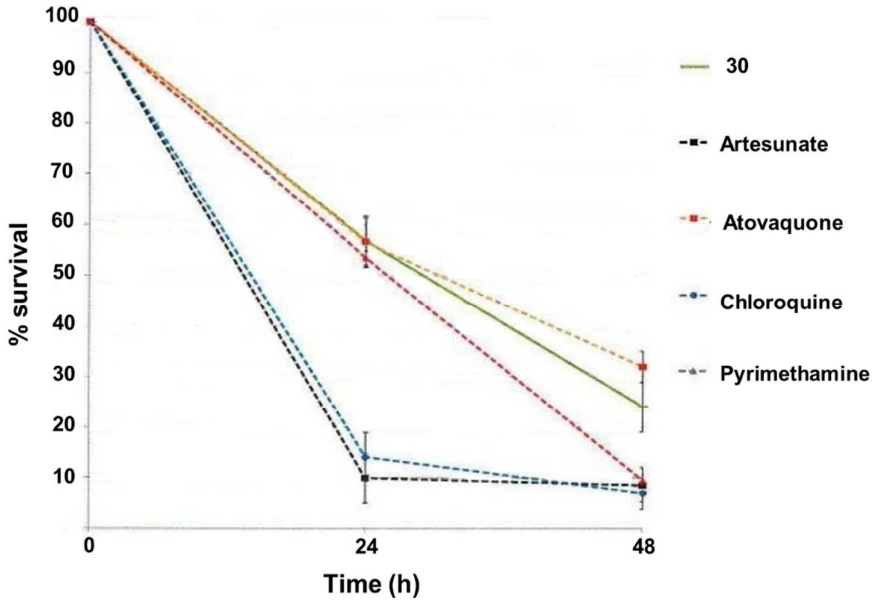

Figure 6: In vitro killing profile of **30** over 48 h

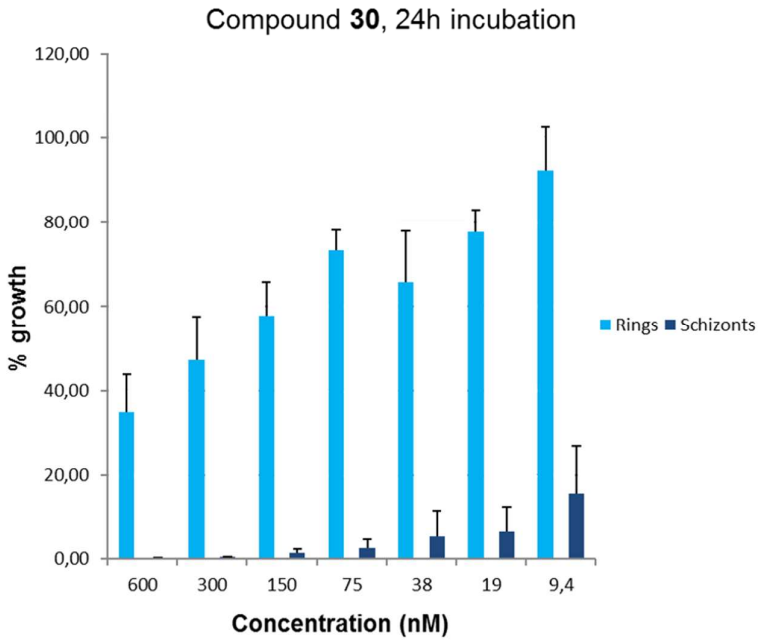

Figure 7: Stage specificity of compound 30 (NF54 synchronized culture; mean of n = ≥2 independent [^{3}H]-hypoxanthine incorporation assays)

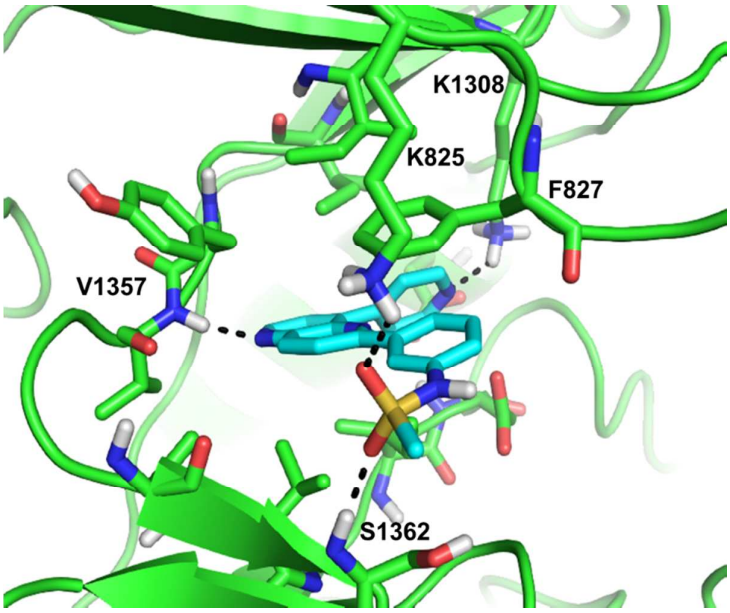

Figure 8: Homology model of *Pf*PI4K showing potential interactions of **26** within the binding pocket

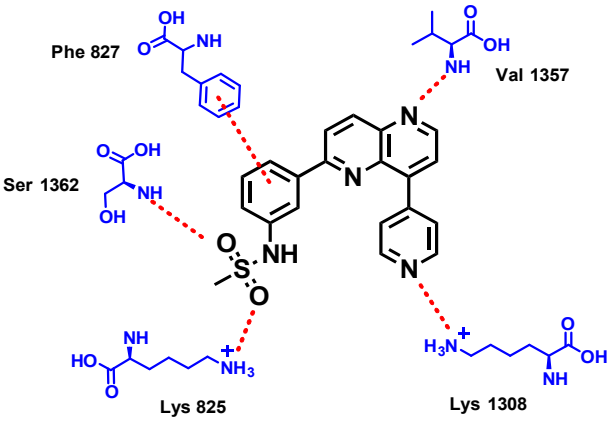

Figure 9: 2D model depicting putative interactions of **26** in the *Pf*PI4K homology model